

Hydrogen effect on shearing and cleavage of Al: A first-principles study

F. Apostol* and Y. Mishin†

Department of Physics and Astronomy, MSN 3F3, George Mason University, Fairfax, Virginia 22030, USA

(Received 10 May 2011; revised manuscript received 16 July 2011; published 6 September 2011)

We report on first-principles calculations of the effect of a (111) hydrogen layer embedded in Al on generalized stacking fault energies and cleavage energy for different choices of the slip and cleavage planes. It is shown that the H layer softens Al against shear by reducing the stable and unstable stacking fault energies relative to pure Al. This finding points to a possible enhancement of plasticity of Al by H. The H layer also reduces the cleavage energy on the (111) plane. The reductions in the cleavage energy and unstable stacking fault energy compensate each other and produce only a moderate change in the Rice criterion of ductile versus brittle fracture.

DOI: [10.1103/PhysRevB.84.104103](https://doi.org/10.1103/PhysRevB.84.104103)

PACS number(s): 61.72.Nn, 61.72.S–, 62.20.F–, 62.20.mm

I. INTRODUCTION

Interstitial impurities such as hydrogen can strongly affect mechanical behavior of metallic materials.^{1–3} In particular, hydrogen can cause a reduction in cleavage energy and enhancement of local plasticity in Al.^{2,3} Previous thermodynamic analysis and first-principles calculations were focused on a decohesion process in which hydrogen atoms are initially present as bulk impurities and can diffuse to the fresh surface to form a certain coverage.^{4–7} In this work we are interested in two aspects that received much less attention in the literature. First we consider a case in which hydrogen atoms initially form a monolayer inside the Al lattice. Our calculations reported below indicate that the formation of such a monolayer out of isolated impurity atoms is energetically favorable. While temperature can destabilize such monolayers by the entropy effect, they may exist at low enough temperatures and could serve as precursors for hydride formation. Second, we are interested in not only cleavage but also shearing of the lattice parallel to the monolayer, resulting in the formation of generalized stacking faults (GSF).

The effect of a H layer on shearing of Al was studied by Lu *et al.*⁸ by first-principles calculations. They computed the (111) γ surface of Al in the presence of a quarter of a monolayer and showed that hydrogen reduces the Al resistance to shearing in both the [11 $\bar{2}$] and [1 $\bar{1}$ 0] directions by up to 50%. In a subsequent paper, Lu *et al.*⁹ further evaluated the effect of the H layer on shearing along the [11 $\bar{2}$] direction and cleavage along the (111) plane. This time they examined different coverages varying from a quarter of a monolayer to a full monolayer. The authors conclude that for low coverages hydrogen enhances the ductile behavior of Al, whereas for a full monolayer it reduces the ductility. However, when studying the full monolayer, Lu *et al.*⁹ employed an initial configuration that was not the ground state. They pointed out that this configuration transformed to a much more stable one when the block was allowed to expand during the relaxation process. Thus the question of the effect of a full hydrogen layer remains essentially open.

Our goal is to revisit the full monolayer case by identifying its most stable structure and using it as the starting configuration for calculations of GSF energies and cleavage energies for different choices of the slip and cleavage planes relative to the H layer. Our first-principles calculation methodology, which is similar to that of Lu *et al.*⁹, is described in Sec. II, followed

by results and discussion in Secs. III and IV. Our conclusions are summarized in Sec. V.

II. METHODOLOGY

The supercell employed in this work was a rectangular block whose edges were parallel to the [11 $\bar{2}$], [1 $\bar{1}$ 0], and [111] crystallographic directions. It contained nine (111) Al layers, with eight atoms per layer (a total of 72 Al atoms).¹⁰ The initial lattice parameter had the equilibrium value $a_0 = 4.045$ Å calculated for bulk fcc Al. The supercell had periodic boundary conditions in the [11 $\bar{2}$] and [1 $\bar{1}$ 0] directions. Two (111) free surfaces were created by adding six vacuum layers in the [111] direction. In all calculations reported below, the cross section of the supercell parallel to (111) was kept constant. However, the atoms could freely expand in the [111] direction. This constraint mimicked the situation that would occur in a very thick Al slab where the bulk lattice constant dictates the lateral dimensions, whereas near-surface layers can freely relax into vacuum.

The first-principles density functional theory calculations were performed with the Vienna *ab initio* simulation package (VASP)^{11,12} using ultrasoft pseudopotentials^{13,14} and the Perdew-Wang generalized-gradient-approximation (GGA-PW91).¹⁵ Previous calculations^{16,17} indicate that the GGA gives more accurate results for the Al-H system than the local density approximation, especially for the site occupation and solution energies of impurity atoms. We used the Methfessel-Paxton smearing method¹⁸ with a smearing width of 0.1 eV and a large cutoff energy of 350 eV. An ($16 \times 16 \times 16$) Monkhorst-Pack¹⁹ k -point mesh sampling the Brillouin zone of the primitive unit cell of bulk fcc Al was scaled for the supercell to a ($4 \times 8 \times 1$) grid. The atomic relaxation was performed using the conjugate-gradient algorithm with a convergence criterion for Hellman-Feynman forces on each atom of 0.02 eV/Å. The energies were convergent to within 1 meV/atom. We note that the calculated equilibrium lattice parameter of fcc Al, 4.045 Å, is in excellent agreement with the experimental value 4.05 Å.

Before studying stacking faults, we checked the interstitial site preference of H in our Al slab by placing a single H atom in the center of the slab in either a tetrahedral (T_d) or an octahedral (O_h) site. The formation energy of a H impurity

ΔE_{imp}^H was calculated by allowing internal relaxation of all atoms:

$$\Delta E_{\text{imp}}^H = E(\text{Slab} + \text{H}) - E(\text{Slab}) - \frac{1}{2}E(\text{H}_2), \quad (1)$$

where $E(\text{Slab} + \text{H})$ is the energy of the Al slab with one H atom located at a T_d or O_h site, $E(\text{Slab})$ is the energy of the slab without hydrogen, and $E(\text{H}_2)$ is the energy of an isolated H_2 molecule. The latter was calculated by placing H_2 in a cubic box with 15 Å sides. Our results, $\Delta E_{\text{imp}}^H(T_d) = 0.702$ eV and $\Delta E_{\text{imp}}^H(O_h) = 0.816$ eV, show that H prefers the T_d site over the O_h site. These results are in excellent agreement with the dilute heats of solution of 0.69 eV (T_d) and 0.82 eV (O_h) computed by Wolverton *et al.*¹⁶ using a 32-atom cubic cell with periodic boundary conditions in all directions.

The next step was to insert a (111) H layer in the Al slab. It is known that the normal stacking sequence of (111) atomic layers in an fcc crystal is ...ABCABC... as shown in Figs. 1(a) and 1(b). A (111) H layer was inserted between two Al layers of types A and B by placing eight H atoms at either T_d or O_h sites. The corresponding configurations are referred to as I and II, respectively. The atomic coordinates of both structures were then fully relaxed. During the relaxation there were no significant displacements of Al atoms parallel to (111), so that the initial stacking of the (111) layers was preserved. However, the interplanar distance between the (111) Al layers surrounding the H layer increased from the initial spacing in pure Al, $d_0 = a_0/\sqrt{3} = 2.334$ Å, to 2.986 Å for configuration I and 2.720 Å for configuration II.

The relaxed energy of configuration I was found to be lower than that of configuration II by 0.6 eV, indicating that configuration I is more favorable. Initially we chose configuration I as the reference configuration for calculations of stacking fault energies. However, shifting all Al layers above the H plane along the $[11\bar{2}]$ direction and allowing relaxation along $[111]$ lowered the total energy of the block. The lowest energy was obtained for a displacement of $(1/3)[11\bar{2}]$ (so-called run-on stacking). In this case, the neighboring Al

layers on either side of the H layer are both in type A positions [Fig. 1(c)]. No further relaxation in the (111) plane was needed because all forces on atoms were found to be smaller than the preset convergence criterion. The two Al layers surrounding the H layer are separated by a distance of 3.544 Å, which is approximately $1.5d_0$. The H layer is located equidistantly between them (at $\sim 0.75d_0$ from each Al layer). We refer to this configuration as configuration III.

The same translations applied to configuration II combined with atomic relaxations along $[111]$ also lowered the total energy. However, the lowest energy, which was achieved for a displacement equal to the partial Burgers vector $(1/6)[11\bar{2}]$, was considerably larger than the energy of configuration III. We thus conclude that it is configuration III that must be taken as the ground state in stacking fault energy calculations.

In view of the significance of the latter finding, the question of a possible role of zero-point vibrations deserves some comment. Due to the high frequency of hydrogen atom vibrations in Al, the zero-point energy (ZPE) can, in principle, make contributions to defect energies in the Al-H system. Nevertheless, Wolverton *et al.*¹⁶ found that ZPE does not change the H impurity preference for the tetrahedral site. Furthermore, although the energetic preference of tetrahedral sites decreases from 0.13 to 0.05 eV when ZPE is taken in account, the migration energy for H between the tetrahedral and octahedral positions is not affected. In fact, the migration energy calculated at 0 K without the ZPE is in good agreement with experimental data.¹⁶ Thus the ZPE does not appear to change the basic energetics of defects in Al-H alloys in a drastic way. It should be noted that the energetic preference of configuration III over the competing configurations I and II is about 500 mJ/m². This is a very large amount of energy on the scale of typical GSF energies (see Sec. III below). It is, therefore, highly unlikely that the energetic preference of configuration III could be an artifact caused by the neglect of the ZPE in our calculations.

For the Al block with a H layer, the formation energy per H atom, $\Delta E_{\text{layer}}^H$, can be computed in a similar way as ΔE_{imp}^H :

$$\Delta E_{\text{layer}}^H = \frac{1}{8}[E(\text{Slab} + \text{H layer}) - E(\text{Slab}) - 4E(\text{H}_2)]. \quad (2)$$

For configuration III we obtain $\Delta E_{\text{layer}}^H(\text{III}) = 0.465$ eV. It is important to observe that this number is smaller than $\Delta E_{\text{imp}}^H(T_d) = 0.702$ eV by 0.237 eV, showing that the formation of a H layer in configuration III out of isolated H impurity atoms is energetically favorable. Each H atom forms strong chemical bonds with the two Al atoms located directly above and below it in the $[111]$ direction, compensating for the increase in energy due to the breaking of the normal ...ABCABC... stacking sequence of (111) Al layers. Applying Eq. (2) to configurations I and II gives the relaxed values of $\Delta E_{\text{layer}}^H(\text{I}) = 0.714$ eV and $\Delta E_{\text{layer}}^H(\text{II}) = 0.801$ eV. Both values are larger than $\Delta E_{\text{imp}}^H(T_d)$ suggesting that these configurations are not energetically favorable over isolated H impurities.

It should be noted that our configuration III is similar to the configuration with the lowest energy found by Lu *et al.*⁹ when they performed volume and atomic relaxation of their initial (1×1) supercell with the H atom located at the T_d site. In our work, configuration III was chosen as the reference

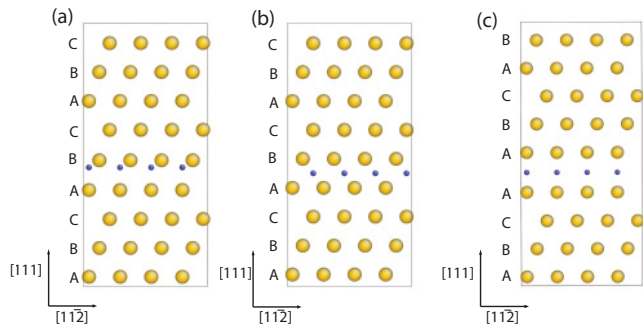


FIG. 1. (Color online) The computational cell employed in this work. The bright (yellow in online version) and dark (blue in online version) spheres represent Al and H atoms, respectively. Letters A, B, and C indicate the type of Al (111) layers in the stacking sequence. (a) and (b) represent starting configurations with H atoms placed at T_d and O_h interstitial positions, respectively. The corresponding relaxed structures are referred to as configurations I and II, respectively. (c) represents the lowest-energy configuration called configuration III. Labels 1, 2, and 3 distinguish between different slip/cleavage planes used in the calculations.

configuration in calculations of the effect of the H layer on shearing and cleavage.

III. GENERALIZED STACKING FAULTS

We now turn to the results for the effect of the H layer on shearing along the $[11\bar{2}]$ direction. The Al layers labeled 1, 2, and 3 are the first, second, and third neighbors above the H layer as shown in Fig. 1(c). If layer 1 together with all Al layers above it are rigidly shifted along $[11\bar{2}]$, then layer 1 is referred to as the slip plane. The same terminology is applied to layers 2 and 3. The distance between the H layer and the slip plane is denoted as D . The GSF energy γ_{GSF} for a displacement x of the upper part of the block relative to the lower part along the $[11\bar{2}]$ direction was calculated as the excess energy per unit area:

$$\gamma_{\text{GSF}}(x) = \frac{E(x) - E(0)}{A}, \quad (3)$$

where A is the cross-sectional area of the block. The energy $E(x)$ was obtained by partial relaxation according to the definition of the γ surface,^{20,21} that is, all atoms were allowed to move only in the direction normal to the fault plane.

Figure 2 shows the GSF energy curves computed for three slip planes: plane 1 ($D = 0.75d_0$), plane 2 ($D = 1.75d_0$), and plane 3 ($D = 2.75d_0$). The corresponding stacking faults are referred to as GSF1, GSF2, and GSF3, respectively. The GSF

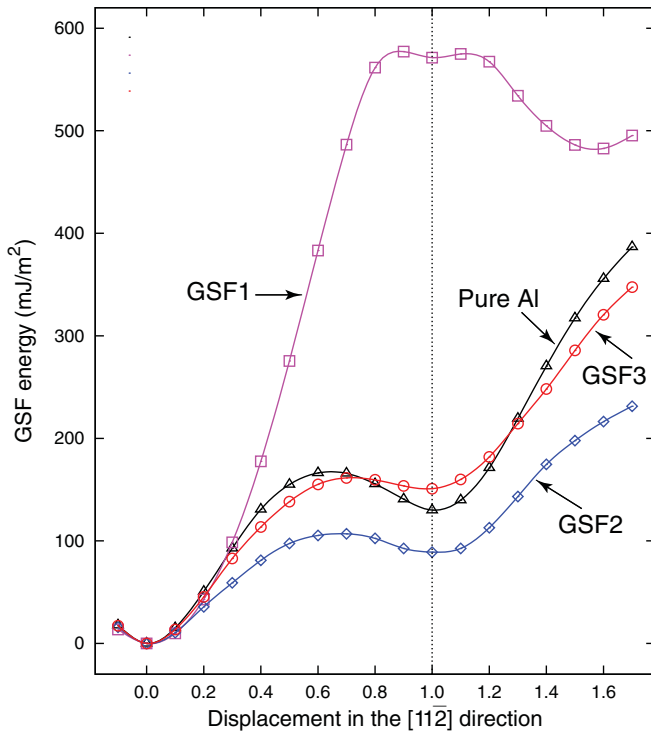


FIG. 2. (Color online) The relaxed generalized stacking fault (GSF) energy curves for shear along the $[11\bar{2}]$ direction computed for Al with and without a H layer for three different slip planes (1, 2, and 3 as described in the text). The distances between the H layer and the slip plane are $D = 0.75d_0$ (GSF1), $1.75d_0$ (GSF2), and $2.75d_0$ (GSF3), where d_0 is the (111) interplanar spacing in pure Al. The displacement along the $[11\bar{2}]$ direction is measured in the units of the partial Burgers vector $(1/6)[11\bar{2}]$.

curve computed for pure Al is included for comparison. The relaxed stacking fault energy in pure Al, $\gamma_{\text{SF}}^{\text{Al}} = 131 \text{ mJ/m}^2$, computed in this work is in good agreement with other first-principles results reported in literature: 147,²² 134,⁹ and 143 mJ/m^2 .²³

As evident from Fig. 2, the GSF1 curve has a totally different shape from that in pure Al. This result is not surprising given that the initial Al stacking sequences at the fault plane are different: ...ABC|ABC... in pure Al and ...ABCA|ABC... in the presence of a H layer (the vertical bar indicates the slip plane). The GSF1 curve has three minima corresponding to the displacements $x = 0$, $x = (1/6)[11\bar{2}]$, and $x = (4/15)[11\bar{2}]$, where $(1/6)[11\bar{2}]$ is the Shockley partial Burgers vector. It should be noted that the shallow minimum at $x = (1/6)[11\bar{2}]$ corresponds to configuration I, which has the same stacking sequence as in pure Al. The corresponding GSF energy $\gamma_{\text{SF}}^{(1)}$ has a large value of 571 mJ/m^2 . The lower minimum at $x = (4/15)[11\bar{2}]$ has a GSF energy of 483 mJ/m^2 , which is still much larger than $\gamma_{\text{SF}}^{\text{Al}}$.

On the other hand, the GSF2 and GSF3 curves have shapes similar to that for pure Al, having only two minima at $x = 0$ and $x = (1/6)[11\bar{2}]$ separated by a maximum corresponding to the unstable stacking fault (Fig. 2). Both the GSF2 and GSF3 curves have flatter shapes around the stacking fault minimum. The smallest GSF energy for the entire range of x values was obtained in the GSF2 case.

The computed stacking fault energies γ_{SF} and unstable stacking energies γ_{us} are summarized in Table I. It is observed that $\gamma_{\text{us}}^{(2)} < \gamma_{\text{us}}^{(3)} < \gamma_{\text{us}}^{\text{Al}} < \gamma_{\text{us}}^{(1)}$ and $\gamma_{\text{SF}}^{(2)} < \gamma_{\text{SF}}^{\text{Al}} < \gamma_{\text{SF}}^{(3)} < \gamma_{\text{SF}}^{(1)}$, where superscripts 1, 2, and 3 indicate the position of the slip plane. We can conclude that when a shear stress is applied in the $[11\bar{2}]$ direction, the shearing of the material in the presence of a H layer should occur along layer 2. The presence of the H layer softens Al for shear, reducing $\gamma_{\text{us}}^{\text{Al}}$ to $\gamma_{\text{us}}^{(2)} = 107 \text{ mJ/m}^2$ (a 36% reduction) and $\gamma_{\text{SF}}^{\text{Al}}$ to $\gamma_{\text{SF}}^{(2)} = 89 \text{ mJ/m}^2$ (a 32% reduction).

By placing the H layer closer to the bottom surface of the supercell, we were able to evaluate the shearing along the fourth and fifth Al planes above the H layer. Although the computed fault energies are affected by the surfaces, the general trend is consistent with expectations: the further away is the slip plane from the H layer, the smaller is its effect on shearing resistance. This trend is illustrated by the plot of the stacking fault energy difference $\Delta\gamma_{\text{SF}}^{(N)} = \gamma_{\text{SF}}^{(N)} - \gamma_{\text{SF}}^{\text{Al}}$, where $N = 1, \dots, 5$, as a function of distance D between the H layer and the slip plane (Fig. 3).

TABLE I. Stacking fault energy γ_{SF} , unstable stacking energy γ_{us} , cleavage energy γ_{cl} , and the ratio $\gamma_{\text{cl}}/\gamma_{\text{us}}$ with and without a H layer in Al computed for different distances D between the H layer and the slip/cleavage plane.

	Pure Al	Al with a H layer		
Slip/cleavage plane		1	2	3
D		$0.75d_0$	$1.75d_0$	$2.75d_0$
γ_{SF} (mJ/m^2)	131	571	89	151
γ_{us} (mJ/m^2)	168	577	107	162
γ_{cl} (mJ/m^2)	1643	1191	1321	1646
$\gamma_{\text{cl}}/\gamma_{\text{us}}$	9.81	2.06	12.36	10.19

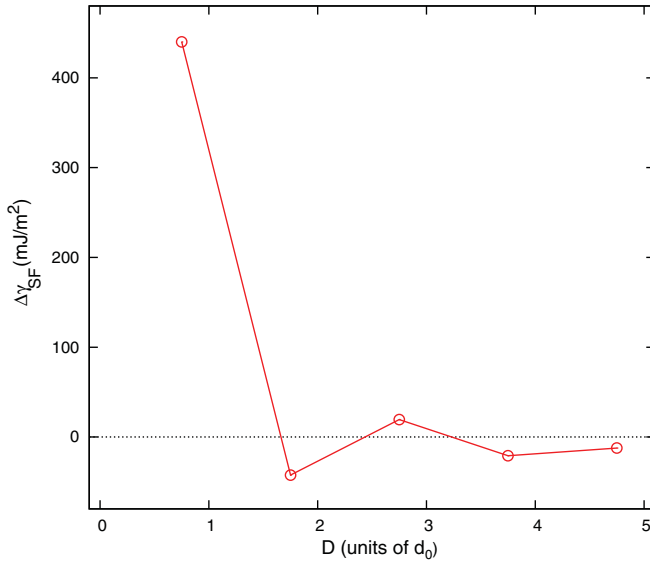


FIG. 3. (Color online) The stacking fault energy difference $\Delta\gamma_{SF} = \gamma_{SF} - \gamma_{SF}^{Al}$ computed for Al with a H layer as a function of the distance D between the H layer and the slip plane. γ_{SF}^{Al} represents the stacking fault energy of pure Al. D is measured in units of the (111) interplanar spacing d_0 in pure Al.

IV. WORK OF DECOHESION

The resistance of a crystal to fracture is characterized by its cleavage energy γ_{cl} defined below. Furthermore, the ratio γ_{cl}/γ_{us} indicates the tendency of the crystal to exhibit brittle or ductile behavior.^{1,24,25} In this work we examined the effect of the H layer on the cleavage fracture energy and the brittle/ductile fracture behavior of Al.

γ_{cl} was computed as the work per unit area required to separate the Al slab in two slabs by creating two new free surfaces with the (111) orientation. For pure Al $\gamma_{cl}^{Al} = 2\gamma_s^{Al}(111)$, where γ_s^{Al} is the surface energy. To compute this quantity, the upper part of the Al slab was separated from the lower part by three (111) layers of vacuum (~ 7 Å) and the atomic coordinates were fully relaxed. The bottom Al layer of the upper slab is referred to as the cleavage plane. Our result for pure Al, $\gamma_{cl}^{Al} = 1643$ mJ/m² [$\gamma_s^{Al}(111) = 821$ mJ/m²] is in reasonable agreement with previous calculations with VASP: 1934 mJ/m² (LDA),⁹ 1680 mJ/m² (LDA),⁷ and 2000 mJ/m² (GGA-PBE).⁷ For the ratio $\gamma_{cl}^{Al}/\gamma_{us}^{Al}$ we obtain the value of 9.81 in good agreement with 10.6 reported by Lu *et al.*⁹

As cleavage planes we chose the same Al layers as were used as slip planes in the shearing calculations. Thus, D also stands for the distance along [111] between the H layer and the cleavage plane prior the splitting of the initial slab in two slabs. The relaxed values of the cleavage energy $\gamma_{cl}^{(N)}$ ($N = 1, 2, 3$) are given in Table I. From the relations $\gamma_{cl}^{(1)} < \gamma_{cl}^{(2)} < \gamma_{cl}^{(3)} \approx \gamma_{cl}^{Al}$, it can be concluded that that cleavage should occur between the H layer and the nearest Al layer (layer 1). Furthermore, the H layer lowers the resistance of Al to cleavage by reducing the cleavage energy from $\gamma_{cl}^{Al} = 1643$ mJ/m² to $\gamma_{cl}^{(1)} = 1191$ mJ/m².

The calculation of $\gamma_{cl}^{(1)}$ required special efforts. Upon separation, the lower slab contains a H layer covering the

Al surface. The adsorbed H atoms are initially on top of the underlying Al atoms (atop sites). Full relaxation of the atomic coordinates was found to reduce the initial cleavage energy to 1323 mJ/m², with H atoms still occupying the atop sites. However, previous first-principles studies^{7,9,26} have shown that for H adsorbed on (111) Al, the threefold fcc coordinated adsorption sites are the most favorable energetically. To verify this we placed H atoms at different high-symmetry sites (atop, fcc, hcp, and bridge) as well as some intermediate configurations, and performed full relaxations of atomic coordinates. The results showed that the configuration in which the H atoms occupied the fcc sites indeed had the lowest energy. We, therefore, assumed that when the initial block is split along layer 1 under real conditions, the H atoms will migrate from the atop sites to fcc sites. Accordingly, the most stable configuration with H atoms filling the fcc adsorption sites was taken as the final surface configuration in calculating the cleavage energy $\gamma_{cl}^{(1)}$.

The ratio of the lowest cleavage energy in the presence of the H layer, $\gamma_{cl}^{(1)}$, to the lowest unstable stacking energy in the presence of the H layer, $\gamma_{us}^{(2)}$, was taken as a measure of the effect of the H layer on the ductility of Al fracture. This ratio was found to be $\gamma_{cl}^{(1)}/\gamma_{us}^{(2)} = 11.14$. It is somewhat larger than the ratio $\gamma_{cl}^{Al}/\gamma_{us}^{Al}$ for pure Al, indicating that the H layer may increase the ductility of Al fracture. However, the effect is only moderate.

V. DISCUSSION AND CONCLUSIONS

We have shown by first-principles calculations that the (111) H layer embedded in Al produces a structural change in the stacking sequence of (111) Al layers. Furthermore, the H layer softens the Al lattice for shear in the [112] direction. Calculations involving different slip planes indicate that when a shear stress is applied in the [112] direction the lattice is most likely to shear along a slip plane which is not nearest, but next nearest to the H layer. Both the stable and unstable stacking fault energies on this slip plane are smaller than on other slip planes and are considerably lower than in pure Al. This points to a possible enhancement of plasticity caused by hydrogen, an effect which was observed in experiments.^{2,3}

At the same time, the work of decohesion is the smallest when the separation occurs between the H layer and the nearest Al layer. We have shown that the decohesion process should be accompanied by a reconstruction in which the adsorbed hydrogen atoms move from the initial atop positions to fcc-type positions on the Al surface.

During the fracture process the competition between cleavage and plastic deformation by generation of partial dislocations is controlled by the Rice factor γ_{cl}/γ_{us} .^{1,24,25} Using the smallest values of γ_{cl} and γ_{us} computed in the presence of the H layer, the Rice ratio obtained (11.14) is only slightly larger than the ratio for pure Al (9.81), suggesting only a slight trend toward more ductile fracture caused by hydrogen.

Our calculations have shown that the formation of a hydrogen layer out of isolated atoms is energetically preferred by about 0.24 eV per H atom. It should be noted, however, that these calculations assumed an infinitely large H layer. Under real conditions, the layer can form by nucleation

of a single-layer disk, which could initially be coherent with the Al matrix. The hydrogen positions within the disk are likely to be in configuration I [Fig. 1(a)], which is readily created by simple aggregation of H atoms without changing their T_d occupation or shuffling the Al layers. The excess energy of configuration I (which corresponds to the highest shallow minimum in Fig. 2) and the elastic stresses in the matrix are responsible for the energy barrier of the disk formation. As the disk grows by continuing diffusion of hydrogen atoms, a moment must come when the atomic configuration will switch to type III. This switch will be accompanied by a large reduction in energy due to the strong energetic preference of configuration III. Note that the barrier of the structural transformation between the configurations I and III is small (Fig. 2). At the same time, the relative shift of the Al layers will create a dislocation loop on the sides of the disk, whose energy will be positive. Since the

dislocation loop energy grows approximately in proportion to the radius of the disk while the total hydrogen energy within the disk decreases as the square of the radius, the latter contribution will eventually win and the disk will continue to grow without a barrier. The proposed nucleation scenario of a hydrogen layer is hypothetical and requires validation by further research.

ACKNOWLEDGMENTS

We are grateful to W. A. Curtin and J. Song for stimulating discussions. We are especially grateful to W. A. Curtin for calling our attention to the problem of hydrogen layer nucleation discussed in the previous paragraph. This work was supported by the National Aeronautics and Space Administration through the Langley Research Center under Grant No. NRA # NNX08AC07A.

*fapostol@gmu.edu

†ymishin@gmu.edu

¹J. R. Rice, in *Effect of Hydrogen on Behaviour of Materials*, edited by A. M. Thompson and I. M. Bernstein (TMS-AIME, New York, 1976), p. 455.

²P. Sofronis and I. M. Robertson, *Philos. Mag. A* **82**, 3405 (2002).

³A. Pundt and R. Kirchheim, *Annu. Rev. Mater. Res.* **36**, 555 (2006).

⁴Y. Mishin, P. Sofronis, and J. L. Bassani, *Acta Mater.* **50**, 3609 (2002).

⁵A. Van der Ven and G. Ceder, *Phys. Rev. B* **67**, 060101(R) (2003).

⁶A. Van der Ven and G. Ceder, *Acta Mater.* **52**, 1223 (2004).

⁷D. E. Jiang and E. A. Carter, *Acta Mater.* **52**, 4801 (2004).

⁸G. Lu, Q. Zhang, N. Kiuoussis, and E. Kaxiras, *Phys. Rev. Lett.* **87**, 095501 (2001).

⁹G. Lu, D. Orlikowski, I. Park, O. Politano, and E. Kaxiras, *Phys. Rev. B* **65**, 064102 (2002).

¹⁰If we were interested in only GSF energies, computational efforts could be saved by using the 1×1 supercell geometry with one Al atom per layer.⁹ However, we also wanted to demonstrate that the formation of a hydrogen layer out of isolated H atoms is energetically favorable. This required accurate calculations of the energy of an isolated hydrogen atom in Al, for which a 1×1 supercell would be unsuitable. To keep the entire set of calculations

internally consistent, we chose the structure with eight atoms per layer despite the associated computational costs.

¹¹G. Kresse and J. Furthmüller, *Comput. Mater. Sci.* **6**, 15 (1996).

¹²G. Kresse and J. Furthmüller, *Phys. Rev. B* **54**, 11169 (1996).

¹³D. Vanderbilt, *Phys. Rev. B* **41**, 7892 (1990).

¹⁴G. Kresse and J. Hafner, *J. Phys. Condens. Matter* **6**, 8245 (1994).

¹⁵J. P. Perdew, J. A. Chevary, S. H. Vosko, K. A. Jackson, M. R. Pederson, D. J. Singh, and C. Fiolhais, *Phys. Rev. B* **46**, 6671 (1992).

¹⁶C. Wolverton, V. Ozoliņš, and M. Asta, *Phys. Rev. B* **69**, 144109 (2004).

¹⁷M. Ji, C. Z. Wang, K. M. Ho, S. Adhikari, and K. R. Hebert, *Phys. Rev. B* **81**, 024105 (2010).

¹⁸M. Methfessel and A. T. Paxton, *Phys. Rev. B* **40**, 3616 (1989).

¹⁹H. Monkhorst and J. Pack, *Phys. Rev. B* **13**, 5188 (1976).

²⁰V. Vitek, *Philos. Mag.* **18**, 773 (1968).

²¹V. Vitek, *Cryst. Lattice Defects* **5**, 1 (1974).

²²F. Apostol and Y. Mishin, *Phys. Rev. B* **83**, 054116 (2011).

²³J. Hartford, B. von Sydow, G. Wahnström, and B. I. Lundqvist, *Phys. Rev. B* **58**, 2487 (1998).

²⁴J. R. Rice, *J. Mech. Phys. Solids* **40**, 239 (1992).

²⁵J. R. Rice and J. S. Wang, *Mater. Sci. Eng. A* **107**, 23 (1989).

²⁶R. Stumpf, *Phys. Rev. Lett.* **78**, 4454 (1997).